

Microanalysis of ferric-ferrous ratio of silicate glasses by visible microspectroscope

OKUMURA, Satoshi^{1*}, Yuta Yamanoi²

¹Dept. Earth Science, Tohoku Univ., ²Konica Minolta Sensing, Inc.

Ferric-ferrous ratio of magma reflects source mantle and evolution of redox state during magma ascent to earth surface (e.g., Kelley and Cottrell, 2009 Science; Burgisser and Scaillet, 2007 Nature). A direct method to determine the redox state is to investigate the ferric-ferrous ratio of quenched glasses in volcanic rocks. The synchrotron micro XANES technique, which has high spatial resolution down to 10 μm (Delaney et al., 1998 Geology), has been applied to the measurement of ferric-ferrous ratio of volcanic glasses, but the major disadvantage of this method is the limited number of facilities. Here, we develop a visible microspectroscope to measure ferric-ferrous ratio of silicate glasses in in-house laboratory and report preliminary results.

The visible microspectroscope consists of a microscope, a halogen lamp unit, and a monochromator. In this system, the intensity of the monochromatic light through a sample thin section is measured using a digital camera with the raw mode. Because we use the monochromatic light and digital camera, two dimensional data can be obtained, which is expected to have high spatial resolution.

We synthesized standard glasses with different chemical compositions (JA3 and JB3) and different ferric-ferrous ratios to calibrate the relationship between ferric-ferrous ratio of the glasses and the transmittance of visible lights. The glasses were prepared by melting powder samples using a Pt wire-loop method, at a temperature of 1300 deg C under $\text{CO}_2\text{-H}_2$ mixed gas flow. On the basis of the CO_2/H_2 ratio, the oxygen fugacity was controlled to be $\Delta\text{NNO}-1$ to $\Delta\text{NNO}+3$, and the ferric-ferrous ratio was calculated from the mixed CO_2/H_2 ratio. The quenched glass was doubly polished to thin sections with thicknesses of approximately 60 and 110 μm . The visible light image of the glasses was obtained using some different wavelengths (420, 440, and 520 nm). The greyscale intensity in 8 bit was measured in different points in the glass and normalized by the background intensity. For the analytical condition of this study, the transmittance of 420 nm shows a good correlation with the ferric-ferrous ratio without intensity saturation. Hence, there is a possibility that the ferric-ferrous ratio and redox state of basaltic to andesitic glasses can be determined using the visible microspectroscope.

We will apply the method established in this study to melt inclusion in pyroclasts to investigate the change in redox state of magma before volcanic eruptions and to examine the relationship between redox state of magma and the injection of fluid into magma chamber which has been recently proposed in many volcanoes (e.g., Blundy et al., 2010 EPSL).

Keywords: silicate glass, ferric-ferrous ratio, visible spectroscopy, magma, mantle, redox state

Bubble number density (BND) from bubble wall

ITAKURA, Matomu^{1*}

¹Faculty of Science, Kobe University

One of the dynamics of volcanic eruption is the expansion of magma volume resulting from its bubbling. Under high pressure condition, volatile such as water and CO₂ melt in the magma. Decompression caused by uprise of magma leads vaporization of the volatile contents which invoke bubble nucleation and expand into bubbles. Bubble number density (BND) is the number of foregoing nucleation per unit bulk volume. BND is proportional to the (3/2) power of the decompression rate as demonstrated by Toramaru(2006), and it may give significant information of the erupting magma in the chamber and the conduit, where observation is difficult.

To calculate BND, various methods have been developed so far. For instance, Toramaru(1990) calculates BND from the distribution of the length of the lines which cross bubbles, Sahagian and Proussevich(1998) calculates it from the distribution of the cross-section size of vesicles. These traditional methods concentrate on the vesicles, thus it is difficult to calculate BND from the fragmented sample such as volcanic ash or volcanic glass. Volcanic ash, however, constitutes more than half of the volcanic ejecta from a pyroclastic eruption, therefore it is also important to gain the information from fragmented samples or bubble wall. This study proposes two methods to calculate BND from bubble wall thickness.

Regarding bubble wall as *a shell covering the vesicle* and assuming bubble cell model proposed by Zhang(1999), the bubble number density N_V is calculated from following formula: $N_V=6(1-P^{1/3})^3/\pi(1-P)d^3$, where P is the porosity, π is the circular constant and d is the mean thickness of the bubble wall (Oki et al., 2004). On another front, presuming bubble wall to be *a board nipped by the vesicle* and assuming a bubble as a sphere, N_V is: $N_V=16(1-P)^2/(9\pi P^2 l^3)$, where l is the mean free path regarding the bubble wall as space and the vesicles as obstacles.

To verify these methods, BNDs are estimated by both these methods and traditional methods from cross-section images of the same pumices. These pumices have various quality: basaltic or rhyolitic material, high or low porosity, and circular or flattened cross-section shape. Comparing these BNDs, they are within a range from 10^{10} to 10^{17} and show a good correspondence. Thus BND can be calculated from bubble wall.

Keywords: bubble number density, bubble wall

The deposition period of Ohachidaira pyroclastic flow of the Taisetsu volcano estimated from the paleomagnetic study

YASUDA, Yuki^{1*}, SATO, Eiichi², WADA, Keiji³, SUZUKI-KAMATA, Keiko¹

¹Graduate School of Science, Kobe Univ., ²Kobe Univ., ³Hokkaido Univ. of Education

Ohachidaira caldera, about 2km in diameter, is located on the summit area of Taisetsu volcano, central Hokkaido. Caldera-forming pyroclastic flows (hereinafter referred to as Ohachidaira pyroclastic flow) erupted about 30 ka (Katsui et al., 1979). Most of Ohachidaira pyroclastic-flow deposits are exposed at north-west to north-east and south-west of this caldera and form the pyroclastic plateau. Those pyroclastic flows consist of pumices, scorias, and banded pumices as essential materials and are classified into two types based on modal analysis and chemical compositions of volcanic glasses of pumice (Wakasa et al., 2006; Sato and Wada, 2011).

There are two different opinions for the activity of Ohachidaira pyroclastic flow in previous works. Katsui and Ito (1976) and Wakasa et al. (2005, 2006) suggested that those pyroclastic flows erupted within a short period of time. However, Metsugi (1985 MS) suggested that those pyroclastic flows erupted not within a short period of time, but within some length of time because of the erosional gap and the loam layer within the pyroclastic flows. Sato and Wada (2011) has the same opinion because of welded part of pyroclastic flow contained in the pyroclastic flows. This study tries to estimate the deposition period of Ohachidaira pyroclastic flow using the progressive thermal demagnetization method that is used for inferring thermal histories and paleomagnetic directions of pyroclastic deposits.

Samples for remanent magnetization measurement were collected from 10 sites. We collected essential materials and welded tuff as samples from 6 sites of non-welded tuff and 4 sites of welded tuff respectively. Individual specimens, 25mm in diameter and 25mm long, were prepared from samples in the laboratory. Most of samples have a single component of remanent magnetization. A site mean direction from each site has a 95% confidence interval less than 10 degrees. This fact suggests that the site mean directions from all sites represent paleomagnetic directions at the deposition time of each pyroclastic flow. The paleomagnetic directions at 10 sites are divided into two directions. While the magnetization of 4 sites has normal polarity and an easterly direction in declination, the magnetization of 6 sites has normal polarity and a westerly direction in declination. The two directions have little difference in inclination, but have a difference of about 45 degrees in declination. However, three 95% confidence intervals of four sites whose magnetization has normal polarity and an easterly direction in declination and the other 95% confidence interval don't overlap each other. They have a difference of about 15 degrees in inclination. According to the figure of the geomagnetic secular variation for the last 11.6 ka in Japan (Hyodo and Minemoto, 1996), it took several thousand years to change the declination about 45 degrees when the rate of geomagnetic secular variation was slow and several hundred years when the rate was fast. The two types of pyroclastic flows are associated with the two paleomagnetic directions.

As explained above, it is suggested that Ohachidaira pyroclastic flow took at least several hundred years to deposit having some dormant periods. Additionally, it is clear that the two types of pyroclastic flows erupted at intervals.

Keywords: paleomagnetism, pyroclastic flow, deposition period, geomagnetic secular variation, caldera, Taisetsu volcano

Experimental study on the textural relaxation of melt foam

OTSUKI, Shizuka^{1*}, NAKAMURA, Michihiko¹

¹Dept. Earth Sci., Tohoku Univ.

Vesiculation and outgassing of ascending magma control the style of volcanic eruptions. In a series of Vulcanian activity, dense lavas are formed in the volcanic craters in the interval between explosions. It is believed that this dense, less-permeable lava caps play a key role to accumulate overpressure within shallow conduits. Detailed mechanism of the lava cap formation is, however, poorly understood. The decrease of permeability in the foamed magma has generally been attributed to the compaction associated with permeable-flow outgassing (Westrich and Eichelberger, 1994, Okumura et al., 2010). The surface tension of melt is a primary force for textural development of vesiculated magmas such as bubble coalescence and textural relaxation (e.g., Saar and Manga, 1999), but its effect on the microstructure, density and permeability of magmas is not well constrained.

We carried out heating experiments of an andesitic pumice (Taisho eruption of Sakurajima volcano in 1914) to examine the process of surface tension-driven foam collapse. Its bulk water content is ca. 0.5 wt.%. We have conducted the experiments in two pressure conditions. One is low water vapor pressure experiment ($0 \text{ atm} < P_{\text{total}} = P_{\text{O}_2}$, $\text{NNO} < 1 \text{ atm}$, LVP), and the other is higher ($P_{\text{total}} = P_{\text{H}_2\text{O}} = 20, 40 \text{ and } 60 \text{ atm}$; HVP). The experimental temperature for the LVPs and HVPs were 400 to 1000 and 1000 deg.C, respectively. The run duration ranges from 0.5 to 32 hours. After the runs, run products were observed with scanning electron microscope (SEM). The geometry of bubble such as vesicularity, circularity, connectivity and bubble size distribution were analyzed on the BSE images. In the LVPs and HVPs at 1000 deg. C, the vesicularity and the connectivity decreased and the circularity increased. At $< 800 \text{ deg. C}$, however, no significant densification was observed. The melt viscosity was calculated to be $10^6, 10^8 \text{ and } 10^{11} \text{ Pa s}$ for the HVPs, LVPs at 1000 and 800 deg. C, respectively. The surface tension was calculated to be ca. 235 m N/m for all the experimental conditions. It is inferred that in the Vulcanian eruptions, the microstructure of the foamed melt quickly relax due to the surface tension of melt, resulting in the formation of impermeable lava caps in the crater.

Keywords: melt foam, surface tension, textural relaxation, permeability, viscosity

Observation of the fragmentation process of the analogous magma in the solid/liquid transition regime

OKABE, Wataru¹, SHIDA, Tsukasa^{1*}, KAMEDA, Masaharu¹, ICHIHARA, Mie²

¹Department of Mechanical Systems Engineering, Tokyo University of Agriculture and Technology, ²Earthquake Research Institute, University of Tokyo

The fragmentation of vesicular magma is a key phenomenon to determine the style of volcanic eruption. To understand the magma fragmentation, we performed a rapid decompression experiment using an analogous material of magma.

We classify the onset of fragmentation using the brittleness defined by Ichihara and Rubin (2010). The results are as follows: (a) Brittle fracture occurs when the brittleness is from 0.9 to 1.0 only if the differential stress reaches the critical stress, and (b) Ductile expansion occurs when brittleness is smaller than 0.9 even if the differential stress is slightly larger than the critical stress. In addition to the classifications (a) and (b), we find the other class: (c) Delayed fracture occurs when the differential stress sufficiently exceeds the critical stress. We focus our attention to the delayed fracture on this report.

The delayed fracture occurs after the relaxation time of viscoelastic material. Moreover, it causes within the characteristic time of bubble expansion in viscous liquid. This means that the delayed fracture is solid-fracture named brittle-like fracture.

The reasons why the brittle-like fracture occurs when the brittleness is much smaller than 0.9 might be (1) increase of the material viscosity as cooling during the decompression, and (2) inner cracks which are made when the bubbles are mixed into the analogous material.

First, we performed the decompression experiments using two thermocouples, one of which is put on the surface of the material and the other of which is placed in the surrounding gas of the material to check over the cooling effect during the decompression. The gas temperature in the decompression device becomes several tens degrees Celsius lower when the initial value during the experiment. On the other hand, the temperature on the surface of the material remains the initial value in the time scale when the fragmentation happens. This result shows that the cooling effect of the material is not a factor of the delayed fracture happen.

Next, we performed the decompression experiments using the materials having various void fractions and which have a constant brittleness and differential stress. The result shows that the higher void fraction the material has, the easier fracture happens. Thus, the growth of inner cracks during the decompression may lead to the brittle-like fracture.

The brittle-like fracture found in this experiment may happen in specific actual volcanic events in which the onset of explosive eruption is remarkably delayed from the time when the decompression occurs.

Keywords: fragmentation, viscoelasticity, analogous experiment, brittleness

Analog experiment for limnic eruption

OHBA, Takeshi^{1*}, Teruhisa Katagiri¹

¹Dep. Chem. School. Sci.

1. Introduction

The explosive discharges of CO₂ gas (= limnic eruption) at Lake Nyos and Monoun killed about 1800 people around the lakes in mid-1980s. The cause of the limnic eruption was the excessive accumulation of CO₂ gas in lake water. The CO₂ gas originated from a degassing magma. A mineralized water containing CO₂ gas is expected to be discharged on the lake floor. The accumulation of the dissolved CO₂ gas facilitated strong stratification of lake water. In this study, laboratory analog experiments were carried out to reveal the elemental process in limnic eruption.

2. Experiments

A (CO₂ dissolution and degassing) In a clear acrylic plastic cylinder vessel, 2L of pure water with pH indicator (methyl red) was placed. The inner diameter and height of the vessel is 150mm and 300mm, respectively. The head space of the vessel was filled with pure CO₂ at 0.2 MPa. After the confirmation of CO₂ dissolution with the color change of solution, the pressure of vessel was reduced to 0.1 MPa within 10 seconds.

B (CO₂ generation with a chemical reaction) A clear acrylic plastic cylinder was prepared for experiment. The inner diameter and height of the cylinder was 94 and 310 mm, respectively. The cylinder can be separated at the position the height of which is 34 mm from the bottom. The upper and lower parts of cylinder can be separated by use of a thin plastic sheet. Inner volume of lower part of cylinder is 235 ml. Two different solutions, 1M HCl and 0.2M Na₂CO₃ were placed in upper or lower rooms of cylinder. By taking off the sheet, the above two solution was reacted.

3. Results and discussion

In the experiment-A, a generation of CO₂ bubbles were observed, however the rate of generation was low, therefore, no convection of solution was induced, because the generated bubble upraised individually. The result suggests the degree of super saturation in terms of CO₂ dissolution was insufficient.

In the experiment-B, when Na₂CO₃ solution was placed in the upper part of cylinder, rapid generation of CO₂ gas happened, and the upper face of the gas-liquid two phase fluid reached near the upper end of cylinder. When HCl solution was placed in the upper part, the reaction between solutions and the generation of CO₂ bubbles was limited, therefore, the convection in solution was not induced. The measured density of Na₂CO₃ and HCl solutions was 1.023 and 1.018 g/cm³, respectively, suggesting the rapid generation of CO₂ gas was triggered by the gravitational descent of heavy solution and subsequent effective reaction between solutions.

Keywords: Limnic eruption, Analog, CO₂

What controls time intervals between volcanic eruptions: Analysis using a magma plumbing model

IDA, Yoshiaki^{1*}, OIKAWA, Jun¹

¹Advance Soft Co., ²Earthquake Res. Inst., Univ. of Tokyo

How long a volcano pauses between eruptive events is a fundamental question for understanding of eruption mechanism and prediction of volcanic eruptions. Eruptions sometimes happen almost regularly with a constant time interval. During the last one hundred years, for instance, Usu volcano erupted about every thirty years and Miyakejima did about every twenty years, informing us about an approximate time of coming eruptions. Even in these two volcanoes, however, natures and magnitudes of eruptions have changed every event and the periodicity of eruptions was sometimes greatly disturbed in earlier events. Furthermore, many of other volcanoes show no evidence for periodic occurrences of eruptions.

Some volcanoes like Kilauea and Etna have frequently erupted with abundant records of when eruptive events happened. It has been pointed out that time sequences of events for these volcanoes do not show presence of any characteristic time like a period but rather a nature of fractal (Dubois and Cheminee, *JVGR* 45, 197-208, 1991). Even in these cases, however, obtained fractal dimensions significantly fluctuate depending on selected time ranges of analysis so that the fractal nature may not have been well established. Unfortunately, only a few volcanoes have sufficient numbers of eruption records to allow a similar analysis.

With this background we have begun to study the controlling factors of time intervals and magnitudes of eruptions using a simple model of magma plumbing system. We may qualitatively interpret periodic occurrences of eruptions simply supposing that a magma chamber that has been fed with magma from below emits magma to the surface when the accumulation exceeds its capacity. One of the authors earlier proposed a more quantitative model in which the exit of the magma chamber opens or closes with viscous deformation responding to magma pressure changes (Ida, *GRL*, 23, 1457-1460, 1996). This model was formulated using a simple set of time-dependent differential equations. The present analysis is based on an improved model and aimed to examine how the periodicity and magnitude of eruptions are influenced by disturbances of the supply from below or magma flow in the upper conduit.

In the model used in the present analysis the chamber can be connected to the flow in the upper conduit that may ascend in various styles, but only a simple case of the uniform flow is considered in the presentation. As in the earlier model it is assumed that magma pressure in the chamber is enhanced elastically with magma accumulation and that the exit to the upper conduit opens or closes viscously following the magma pressure. Furthermore, it is newly assumed that the viscosity that controls the exit deformation increases sharply with an exponential dependence as the exit narrows. This magma plumbing system has effectively periodic solutions of magma effusion when magma is supplied from below at a constant rate and the flow in the upper conduit is uniform. In this periodic solution, the time interval between eruptions is shorten almost in reciprocal proportion to the supply rate from below while the erupted mass increases and the peak eruption rate slightly decreases as the supply rate is greater.

In the presentation we examine how the eruptive flow is influenced by a periodic change of the supply from below. According to results of the numerical simulation, when the period of the supply change is same as or shorter than the characteristic period of eruptions, the periodicity of surface eruption is little influenced even if the period is slightly longer and the maximum eruption rate is slightly smaller. On the other hand, when the given disturbance has a sufficiently longer period than the characteristic period of eruptions the period and magnitude of eruptions change concordantly with the supply change. Only between these two cases the eruption process is disturbed irregularly with random changes of time intervals and eruption rates.

Keywords: volcanic eruption, periodicity, magma, magma chamber, magma plumbing system, computer simulation

Effects of gas escape and crystallization on a transition from lava-dome to explosive eruption

KOZONO, Tomofumi^{1*}, KOYAGUCHI, Takehiro²

¹NIED, ²ERI, Univ. of Tokyo

During lava dome eruptions, the degree of gas escape and that of crystallization strongly affect the dynamics of conduit flow. Generally, the dynamics of conduit flow is determined by the relationship between chamber pressure p_{ch} and mass flow rate q for steady conduit flow (“the p_{ch} - q relationship”). When the slope of the p_{ch} - q relationship (dp_{ch}/dq) has a positive value (“positive differential resistance”), the steady flow is stable. When dp_{ch}/dq has a negative value (“negative differential resistance”), on the other hand, complex dynamics such as abrupt change and/or cyclic change of magma discharge rate can result. In this study, on the basis of an one-dimensional conduit flow model, we investigated how the coupled effects of gas escape and crystallization control the features of the p_{ch} - q relationship and transitional process of conduit flow induced by the negative differential resistance.

For conduit flow involving gas escape and crystallization, two positive-feedback mechanisms that result in the negative differential resistance are identified. First, effective magma viscosity decreases with increasing q because of delay of crystallization, leading to the reduction of viscous wall friction (feedback 1). Second, magma porosity increases with increasing q because of less efficient gas escape, leading to the reduction of gravitational load of magma (feedback 2). These two feedback mechanisms induce a sigmoid p_{ch} - q relationship for some realistic conditions; the positive differential resistance in the low- q and high- q regimes, and the negative differential resistance in the intermediate regime. Stable solutions of conduit flow in the low- q and high- q regimes are characterized by low- and high-porosities at vent, corresponding to a stable lava-dome eruption and an explosive eruption, respectively. The analyses of time-dependent conduit flows indicate that, because of the sigmoid p_{ch} - q relationship, magma discharge rate abruptly increases from the low- q to high- q regimes as magma supply at depth gradually increases from the low- q regime to the intermediate regime. We consider that this abrupt increase in magma discharge rate accounts for the transition from a lava-dome eruption to an explosive eruption.

We found that the governing mechanism for the transition from a lava-dome eruption to an explosive eruption changes depending on phenocryst content of magma. For high phenocryst content (volume fraction >0.5), the feedback 1 is the main mechanism that forms the negative differential resistance. In this case, the transition from lava-dome to explosive eruption occurs when the magma supply rate at depth exceeds a fixed critical value. On the other hand, for low phenocryst content (volume fraction <0.5), the feedback 2 plays a key role so that the transition is controlled by the permeability of the surrounding rocks; the critical magma supply rate remarkably decreases with decreasing permeability. The transition due to the feedback 2 is associated with a change in chemical composition of volcanic gas, a drastic increase in magma porosity from nearly 0 to greater than 0.8, and overpressure at a shallower level, which can be detected from geochemical and geophysical observations.

Keywords: lava dome eruption, conduit flow, numerical model, transition of eruption, gas escape, crystallization

The radiography of the latest lava dome in Unzen by cosmic muons

MIYAMOTO, Seigo^{4*}, C. Bozza¹, N. D'Ambrosio¹, G. De Lellis¹, M. Nakamura³, H. Shimizu², H. Tanaka⁴

¹INFN, Italy, ²Kyushu university, ³Nagoya university, ⁴ERI, University of Tokyo

It is significant for the growth model of volcano which has viscous magma to investigate the density structure in a lava dome. The project imaging the new lava dome density structure in Unzen, Japan, is going on. The first observation of the imaging a inner density structure in lava dome with cosmic-ray muon was performed by Tanaka et al. (2007) in Showa-shinzan, Japan. The results indicates the growth model advanced by I. Yokoyama in 2002 is most compatible.

The latest lava dome in Mt. Unzen was formed in the eruption from January 1991 to early 1995 and the activity was calmed down in 1995. The formation of the lava dome in Unzen can be divided into two characteristic growth period, exogenous and endogenous. The exogenous dominant period is from January in 1991 to late 1993, the endogenous dominant period is from the end of 1993 to early 1995. Nakada et al (1995) observed that the surface of the lava dome was moving from the in endogenous period in Unzen. They also observed there are several faults, cracks, and thrusts around the base of lava dome. They proposed a growth model in the endogenous period in Unzen, which is based on their observation and the model includes "peel" structure .

According to the dome growth model by Nakada et al, the current density structure in the lava dome should be the following : 1. The ellipsoidal massive part is in the center of lava dome. 2. The talus spread around the massive ellipsoidal. In the talus region, there are a lot of air gaps, which makes the clear contrast in the image of density with muon-radiography.

The systematic analysis of efficiency and random noise ratio are performed by taking a pattern match and making a connection of muon tracks between three films. After estimation and removing unwanted low energy electron tracks, the density map of Unzen lava dome was calculated. The performance of the detector and the first result of radiography will be shown in this topic.

Keywords: volcano, Unzen, muon, nondestructive, lava dome, eruption

Line-Array infrasound observation for volcanic eruptions at Sakurajima volcano

YOKOO, Akihiko^{1*}, SUZUKI, Yujiro², IGUCHI, Masato¹

¹AVL, Kyoto Univeristy, ²ERI, University of Tokyo, ³DPRI, Kyoto University

As strikingly underlined by the recent Eyjafjallajokull, Grimsvotn, and Puyehue eruptions, once a enormous volume of ash is ejected social and economical activities in the vast areas, not only the proximal area from the volcanoes, become much sluggish. One of the reasons of this problem is vulnerability of aviation to ashes suspended in the air. We have to carefully monitor and mitigate the significant volcanic ash hazard to aviation. Infrasound observations can make a contribution of this construct; for example ASHE project (Garces et al., 2008EOS) make a clear the feasibility of acoustically detecting significant atmospheric ash emissions quantitatively (Fee et al., 2010JVGR) and rapidly notifying civil defense authorities. On the other hands, spectral features of infrasound signals from Vulcanian and Plinian eruption columns have a similarity to that empirically-derived from experiments of pure-air jets (Matoza et al., 2009GRL). They concluded that we may be able to estimate volcanic jet parameters such as the expanded jet diameter and velocity, volume flux, fluid composition, and vent over-pressure from broadband acoustic recording in the future. However, to date it is not sufficiently clear to substantial relations associated with the infrasound signals to behaviors of volcanic columns. Features of infrasound characteristics for various eruption column dynamics and the accurate source of locations in the columns should be investigated first. Therefore, we conducted a line-array observation for infrasound waves of eruptions at Sakurajima volcano during the last half year of 2011.

Eruption activity of Sakurajima volcano is comparatively high in Japan. Showa crater at the southeastern flank of the volcano have begun erupting since 2006 are now in the stage of intermittent small-scaled Vulcanian eruptions. Numbers of the eruptions in 2010 were counted to about 1000 reported by Japan Meteorological Agency. Minor scaled eruptions and ash emissions are almost always continues. Even when no eruptive phenomena are recognized in the crater, large sounds related to gas-exhausting often could be heard. These varieties of scale of eruptions and surface phenomena provide us a suitable field for infrasound observations. The array we used at Sakurajima was composed of 5 microphones with 3 data-loggers (1kHz sampling), and additional 4 sets of microphone and data-logger (200Hz sampling) was also used for a few days on December 2011. Results of our observations revealed several basic but suggestive facts for the future study of volcanic infrasound; for example, the first 10 s duration of the infrasound signal is made by explosion itself. Clear height change of the source from the crater altitude was not identified though slight differences were associated with breach of eruption column. Diffraction and reflection waves are dominant from characteristic topography around Sakurajima volcano, like a wall-like topography of the Aira caldera, after that time, which indicates that accurate characters of infrasound waves radiated from the column itself would be hidden by the strong explosive signals. Adequate new analytical methods will be developed to retrieve the information of pure infrasound signals from such polluted ones.

A combined model of conduit flow and eruption cloud dynamics. Part 4. Internal structure of eruption cloud

KOYAGUCHI, Takehiro^{1*}, SUZUKI, Yujiro¹

¹Earthquake Research Institute, University of Tokyo

In order to predict the transition of eruption styles (e.g., plinian eruption to pyroclastic flow) during explosive volcanic eruptions on the basis of geophysical observations such as ground deformation around erupting volcanoes, we are developing a combined model for conduit flow and eruption cloud dynamics. We consider a conduit which flares with a certain opening angle at the vent, and systematically investigate the dynamics of conduit flow and eruption column using a 1-D steady conduit flow model (Koyaguchi, 2005; Koyaguchi et al., 2010) and 3-D eruption cloud model (Suzuki et al., 2005). We attempt to determine the condition of the generation of pyroclastic flow (column collapse condition) as a function of geological parameters such as pressure in magma chamber and crater shape on the basis of this combined model.

When magma properties (e.g., water content and temperature) are fixed, the column collapse condition has been considered to depend primarily on magma discharge rate (e.g., Carazzo et al., 2008). Koyaguchi et al. (2010) proposed that the column collapse condition also strongly depends on the crater shape. In Part 3, we confirmed this proposition using the 3-D numerical simulations, and showed that the column collapse condition can be roughly estimated from the 1-D steady decompression model at the crater (Woods and Bower, 1995; Koyaguchi et al., 2010) and the 1-D steady eruption column dynamics model (e.g., Bursik and Woods, 1991). In this presentation, we investigate internal structure of eruption cloud by means of 3-D numerical simulations in order to support this conclusion.

According to Koyaguchi et al. (2010), the flow in/above the crater is divided into 4 regimes in the parameter space of radius and pressure at the crater top (the r-p space): (1) sonic flow choked at crater top, (2) under-expanded supersonic flow, (3) over-expanded supersonic flow, and (4) subsonic flow. The boundary between (2) and (3) is defined as correctly expanded supersonic flow. For a given mass discharge rate, the flow regime changes from (1) to (4) as the radius increases and the pressure decreases at the crater top. The eruption columns of the flow regimes (1) and (2) accelerate due to decompression just above the crater, whereas those of the flow regime (3) decelerate at a series of shock waves; as a result, the eruption columns of flow regime (3) are more likely to collapse and generate pyroclastic flow for a given magma discharge rate.

The 3-D simulation results show that the internal structure of eruption cloud has distinct features between under-expanded supersonic flow (regime (1) or (2)) and over-expanded supersonic flow (regime (3)). The under-expanded flow regime is characterized by barrel shocks and Mach disk shock. The axial part of the under-expanded supersonic flow decelerates at the Mach disk shock, whereas an annular supersonic up-flow develops at the edge of jet above the Mach disk shock. The instability in the annular supersonic up-flow enhances mixing between ejected material and ambient air, and hence, stabilizes the eruption column. The over-expanded flow regime, on the other hand, is characterized by oblique shocks; the supersonic flow from the crater decelerates at these oblique shocks, and a region of subsonic flow develops around the jet. In the transitional state between eruption column and pyroclastic flow, this annular subsonic flow partly collapses and generates a small-scale pyroclastic flow, while the central part of the jet forms a stable buoyant eruption column.

Keywords: eruption cloud, conduit flow, numerical simulation, compressible fluid dynamics

Estimation of exit velocity of a volcanic eruption column by a vortex ring model

SUWA, Hiroyuki^{1*}, SUZUKI, Yujiro², YOKOO, Akihiko¹

¹Graduate School of Science, Kyoto univ., ²ERI University of Tokyo

Exit velocity of volcanic eruption column is one of basic and important parameters for understanding of eruption dynamics because it reflects a condition of magma fragmentation and governs eruption cloud dynamics. However, it is difficult to estimate it accurately from eruption images by a simple analysis such as tracking characteristic points of the column. Most of previous imaging studies of eruption columns merely estimated rise velocity and/or surface velocity. Meanwhile, an eruption column has one characteristic feature that has scarcely been remarked; a large vortex structure at the head of the column observed in the early stage (e.g., Patrick, 2007, JGR) is similar to a vortex ring. Detailed quantitative data on vortex rings have been given by many researchers, the relation between vortex ring and exit velocity in starting jet has been investigated (e.g., Gao and Yu, 2010, JFM). In this study, we investigated whether this relation is applicable to a volcanic column, and then we estimated the exit velocity of an eruption column in Sakurajima based on the relation.

In a starting jet ejected from a circular nozzle, the boundary layer separates at the nozzle edge and rolls up to form a toroidal structure at the head of the jet, which is known as a vortex ring. The leading vortex ring is growing by absorbing the trailing jet and travels downstream. As shown in previous experimental investigations using a piston, characteristic parameters of the vortex ring (ring radius, translational velocity, circulation, and ring core radius which is radius of the section of the ring) depend on the nozzle diameter and the piston stroke tU (t : time, U : the exit velocity with the piston). Gao and Yu (2010) have derived $dC/dt=1/2U^2-Uu$, where C is circulation, U is exit velocity, and u is translational velocity of vortex ring. This equation is based on the assumptions that exit velocity is constant and that trailing jet velocity is equal to the exit velocity. This equation enables us to estimate U when dC/dt and u are known.

We used results of 3-D simulations of volcanic eruption columns, so as to ascertain whether the GY equation is applicable to the columns. We made calculations for three cases of exit velocities (67m/s, 134m/s, 201m/s) based on 3-D numerical model of Suzuki et al. (2005, JGR). Fully developed vortex structures were recognized at the head of columns up to heights of 500-1000 m in results of all cases. We measured the height of the vortex ring for each time point, and then we estimated the rise velocity as the translational velocity u . Moreover, we measured the vortex core radius and the surface velocity of the vortex ring for each time point, so as to estimate the circulation of the vortex ring C and the time variation of the circulation dC/dt . As a result, we could obtain the exit velocities within 80-125 % range of the true values from u and dC/dt by the GY equation. Therefore we confirm that exit velocity of an eruption column could be estimated by analyzing the vortex ring.

Employing the same procedures described above, we estimated exit velocity for the Feb. 15 eruption of Sakurajima in 2011. This eruption had the maximum column height of 2-2.5 km from the vent, which was a relatively larger event in Sakurajima, 2011. A vortex structure at the head of the column was clearly recognized up to 1-1.5 km over the vent. Thereafter, the vortex structure stagnated and separated from the main column, and then gradually collapsed. The exit velocity of Sakurajima eruption column was estimated at 40-60 m/s by considering some ambiguity. These exit velocities are lower among the common values in vulcanian eruption (several tens-400 m/s). This means that the pressure at the magma fragmentation was relatively low and the explosion was weak. The analysis of vortex structure is useful for discussing vulcanian eruption mechanisms.

3-D numerical simulations of eruption clouds: Effects of the environmental wind on column height

SUZUKI, Yujiro^{1*}, KOYAGUCHI, Takehiro¹

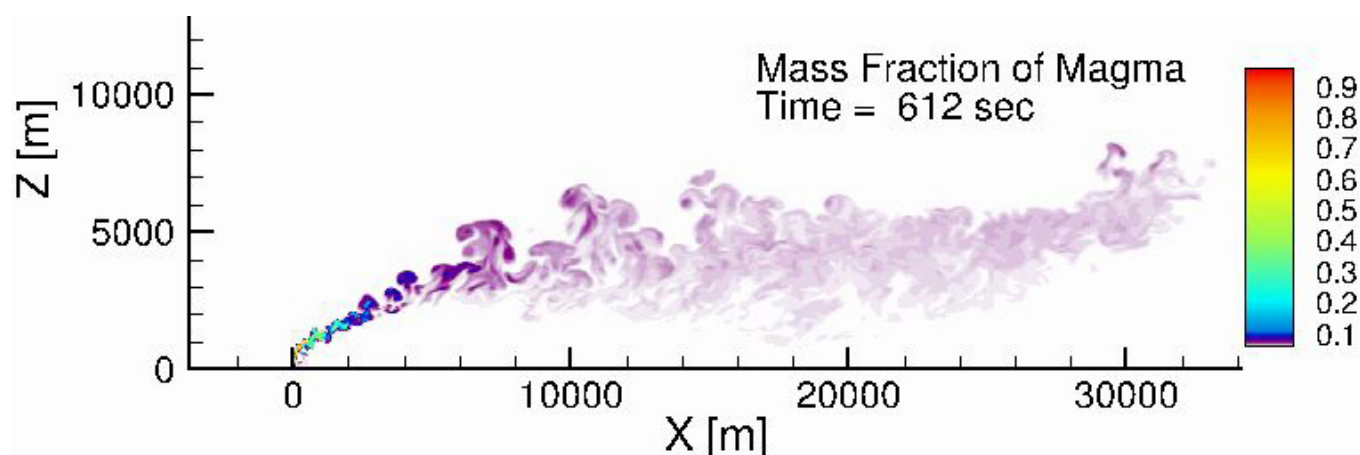
¹ERI University of Tokyo

During an explosive volcanic eruption, an eruption cloud which is ejected from volcanic vent with a high temperature becomes buoyant to generate an eruption column. The heights of eruption column are key observable data for understanding the dynamics of eruption cloud and estimating the eruption conditions at the vent. Therefore, to clarify the relationship between the column height and eruption conditions has been one of the most important issues from the viewpoint of disaster prevention as well as volcanology. Woods [1988] proposed a steady vertical 1-D model of eruption column in a calm environment. This model predicts the column height ($H_{no-wind,1D}$) when the atmospheric condition, the magma properties (temperature and water content), and the eruption conditions (mass discharge rate and exit velocity) are given. Bursik [2001] proposed a steady 1-D model in which the effect of environmental wind is taken into account. This model predicts that the column height in the wind field ($H_{wind,1D}$) is lower than those without the wind ($H_{no-wind,1D}$). In the Shinmoe-Dake 2011 eruption, the column heights in a wind field were accurately measured by means of the weather radar system. The observed column heights are inconsistent with the predictions by the 1-D models ($H_{no-wind,1D}$, $H_{wind,1D}$). In this study, we aim to develop a 3-D numerical model that can quantitatively reproduce column heights in a wind field, and to study the effects of wind on column height.

Using a 3-D unsteady model of eruption cloud [Suzuki et al., 2005], we carried out a numerical simulation of Shinmoe-Dake 2011 26-27th Jan eruptions. The wind velocity, density, pressure, and temperature on the basis of the NHM model [JMA] are applied to the atmospheric condition. On the basis of the petrological data, the magma temperature and water content are assumed to be 1000 K and 3 wt.%, respectively. The average mass discharge rate can be estimated to be 10^6 kg/s from the observation by the tilt-meter. The 3-D model successfully reproduces the eruption column which is strongly bent-over by the environmental wind. The total height of eruption column shows quantitative agreement with the observation.

In order to investigate the effects of wind on column height, we carried out some simulations for variable wind profiles and compared the 3-D simulation results with the 1-D predictions (i.e., $H_{wind,1D}$). The results show that the total height of eruption column in all the cases of the 3-D simulations are higher than $H_{wind,1D}$. Some cases show that the central axes of horizontal flows are consistent with $H_{wind,1D}$, whereas others show that the central axes are higher than $H_{wind,1D}$. These results indicate that the column height depends not only on the average wind speed but also on the wind profile. It is suggested that the basic physics of eruption column dynamics (e.g., the effect of wind on entrainment coefficient) should be systematically studied in order to quantitatively predict the column height in a wind field.

Keywords: volcano, eruption cloud, numerical simulation, turbulent mixing



The Mechanism of the 1888 Phreatic Explosion at Bandai Volcano Part 4: A Second Thought of Visual Data

HAMAGUCHI, Hiroyuki^{1*}, UEKI, Sadato²

¹Free, ²Graduate School of Science, Tohoku Univ.

The eruption at Bandai volcano in 1888 has been known as one of the most gigantic phreatic explosions. Sekiya and Kikuchi (1890) reported that the phreatic explosions occurred almost simultaneously to the directions of up-, north- and southeast-wards. They explained that the phreatic materials stored beneath Kobandai-san and that the flows of outburst happened at the same place and took merely different routes. Recently, Yonechi (1988) analyzed the locations of the outlet of phreatic plume based on the photograph issued by Aizu-wakamatsu-shi (1966). However, this photograph could not used to recognize an existence of other plume due to a deterioration of the picture. Takemoto (2002) suggested a possibility of another huge pheatic plume behind Mt. O-bandai-san, based on the newly discovered photograph with good state of preservation.

In this study, we analyze three old photographs which were taken immediately after the eruption and give the second thought on the 1888 explosion process. On Takemoto's (2002) photograph together with that of Fukushima-Mimpo-sha Company (1988), we identify the third steam plume with a gentle activity and probably with a low-temperature that was issued out at the old crater (Numano-taira). We discuss the physical meaning of vertically discharged steam columns from the old crater and the last explosion projected almost horizontally towards the north, together with the above mentioned observations and also with our explosion model that the pressurized chamber is located just beneath Numano-taira (Hamaguchi and Ueki, 2012).

Keywords: Bandai volcano, phreatic explosion

High temperature uniaxial deformation experiment for Sakurajima Showa Lava

ISHIBASHI, Hidemi^{1*}, MIWA, Takahiro², HIRAGA, Takehiko¹

¹ERI, Univ. Tokyo, ²Geophysics, Science, Tohoku Univ.

Flow law of magma is a critical property to understand magma dynamics during eruption. The effects of suspended crystals on flow law of magma is especially important because suspended crystals induce viscosity increase and non-Newtonian behavior of magma with increasing crystallinity, which results in rheological transition of magma. However, our knowledge about the effects of suspended crystals on flow law of magma, especially those under high crystallinity condition, is not enough despite of recent efforts. In this study, we performed a high-temperature deformation experiment for natural lava to understand the effects of suspended crystals on flow law of high-crystallinity magma.

In this study, Showa lava effused by 1946 eruption at Sakurajima volcano was used for a starting material. The volcano effuses lava flows at least five times in historic times, and the Showa lava is the latest one. The lava sample is two pyroxene andesite, contains ca 60 vol.% of crystals (phenocryst and groundmass crystal) and ca. 10 vol.% of vesicles. High-temperature uniaxial compression experiment was done for the lava using the uniaxial deformation apparatus at Earthquake Research Institute, the University of Tokyo. Experimental conditions are as follows; temperature from 1024 to 886 degree C, strain rate from $10^{-2.4}$ to $10^{-5.5}$ s⁻¹, and atmospheric pressure.

Under present experimental conditions, apparent viscosity of the lava varies from ca. $10^{-7.8}$ to $10^{-11.8}$ Pa s. Apparent viscosity systematically increases as temperature decreases. In addition, shear thinning behavior (apparent viscosity decrease with increase of strain rate) is observed at each temperature. Log apparent viscosity linearly correlates with log strain rate with the slope of -0.505 (1sigma = 0.06). At constant strain rate, log apparent viscosity shows linear relation with reciprocal temperature; apparent activation energy was estimated to be ca. 1.7 kJ, which is similar to that of silicatemelt in Showa lava at the same temperature range. This may suggest that the temperature-dependence of apparent viscosity of the lava is attributed to that of the silicate melt. The ratio of measured bulk viscosity to that of the melt (relative viscosity) increases from $10^{2.7}$ to $10^{4.4}$ as strain rate decreases from $10^{-2.5}$ to $10^{-5.5}$ s⁻¹. Because silicate melt behaves as Newtonian fluid under our experimental conditions, the strain rate-dependence of interaction among crystals may be responsible to the shear thinning behavior. We will perform quantitative textural analyses of our deformed run samples and examine the relation between flow law and texture of the lava.

Keywords: magma, rheology, Sakurajima volcano, non Newtonian, crystal, viscosity

States of magma chamber of Shinmoe-dake, Kirishima Volcano as inferred from steady flow conduit model

TANAKA, Ryo^{1*}, HASHIMOTO, Takeshi²

¹Graduate School of Science, Hokkaido University, ²Faculty of Science, Hokkaido University

1. Introduction

Transition from explosive to effusive eruptions is sometimes seen (e.g. Mt. Pinatubo 1991-92, Mt. St. Helens 1980-86). Some recent studies have discussed the mechanism of such transition of eruption regime (e.g. Kozono and Koyaguchi, 2009; Woods and Koyaguchi, 1994). Also in the 2011 event of Shinmoe-dake Volcano, a sequence of sub-Plinian eruptions was followed by lava effusion within the summit crater. In this study, we applied the 1D steady flow model of Kozono and Koyaguchi (2010) to the dome-forming stage to infer the condition of magma chamber to lose explosivity. This eruption event may fit well to physical model approach since discharge rate, and location of the magma chamber are known from observations and some other important parameters regarding the magma property are also being investigated by some geological and petrological studies. The model which we used here assumes two-phase (liquid-vapor) isothermal magma flow in a cylindrical conduit with vertical gas escape. Dependence of magma viscosity on volatile and crystal content is taken into account.

2. Results and Discussion

First, we made systematic numerical tests by using the above-mentioned model to examine how the initial H₂O content, discharge rate, temperature and conduit radius affect the occurrence of magma fragmentation in the conduit. Then we investigated the upper limit of the initial H₂O content to realize a dome-forming eruption, assuming a discharge rate of 40 m³/s under the temperature range of 950-1050 C (Suzuki et al., 2011; Miyagi et al., 2011), for a conduit radius of 10-50 m. We obtained the upper limit of the initial H₂O content as 1.5-3.8 wt% when the conduit radius is 10 m. Wider conduit gives smaller content of H₂O. This result suggests a release of volatile from the magma chamber during the early stage of the eruption when compared to 3-4 wt%; the initial H₂O content before the sub-Plinian eruptions which is estimated from petrological study (Suzuki et al., 2011).

Even for the non-linear system which has multi-steady states, the pressure of magma chamber is uniquely determined if a discharge rate and a conduit length are given. Herein, we assume 6-8 km for the conduit length as inferred from GPS observation (NIED, 2011; JMA, 2011; GSI, 2011). and the same values of discharge rate and temperature referred above. Applying the upper limit of the initial H₂O content for the dome-forming eruption, we obtain the chamber pressure for the effusive stage which is not so deviated from the pre-eruptive pressure estimation by some petrological studies. This result implies that the degree of pressure decrease due to the sub-Plinian eruptions was not very large, though the deflating ground deformation itself was clearly recognized in GPS records. It may be an implication for the possible size of the magma chamber as discussed below.

It is generally difficult to estimate the volume of a magma chamber by geophysical monitoring. For instance, it is the change in volume, not size of chamber, which is obtained from ground deformation. We here try to estimate the chamber size in two ways. Firstly, the chamber volume is assessed from the relationship between the observed amount of discharged gas during the explosive and the decreased amount of H₂O content in the chamber which is calculate in this study. The other way to estimate the chamber volume uses the the relationship between changes in the chamber pressure and volume at a given rigidity of host rock.

The latter estimation is found to be significantly larger than the former one. This apparent contradiction might be well explained by introducing a conceptual model of a non-uniform magma chamber. For example, a portion of the magma chamber, most plausibly the upper part of it, is efficiently degassed through the sub-Plinian eruptions and loses its explosivity to result in the subsequent dome-forming eruption, while the degree of pressure change is determined by the whole size of the chamber.

Development of low noise calorimeter type cosmic ray muon detector to image internal structure of Usu volcano

KUSAGAYA, Taro^{1*}, TANAKA, Hiroyuki¹, TAKETA, Akimichi¹, OSHIMA, hiromitsu², Tokumitsu Maekawa²

¹ERI, University of Tokyo, ²Usu Volcano Observatory, Hokkaido University

We are now developing a low noise calorimeter type cosmic ray muon detector to image internal structure of Usu volcano with cosmic ray muon radiography. Usu volcano has often erupted and formed upheavals such as Oo-usu, Ko-usu, Ogari-yama, and Usu-shinzan. But the conduits of these are unspecified. Thus, we intend to find out the internal structure of Usu volcano with cosmic ray muon radiography.

Cosmic ray muon radiography of volcano has been performed several times: Mt. Asama (Tanaka et al., 2007, NI&M A; Tanaka et al., 2007, EPSL; Tanaka et al., 2009, GRL; Tanaka et al., 2010, JGR), Showa-Shinzan (Tanaka et al., 2007, GRL), and Satsuma-Iwojima (Tanaka et al., 2009, GRL). These cosmic ray muon radiographies had been performed between only a few hundred meters to one kilometer of muon penetrating length of volcanoes. Because the cosmic ray muon flux penetrating through a few kilometers of rock is two or more order of magnitude less than that through a few meters of rock, signal-to-noise ratio becomes worse and therefore we cannot properly determine the density structure.

In order to investigate Usu volcano conduits, we need a better signal-to-noise ratio detector for accurate measurement of cosmic ray muon flux penetrating through a few kilometers of rock. So we are now developing a calorimeter type muon detector that is thought effective for reducing noise. The calorimeter type muon detector consists of several position-sensitive detectors. A position-sensitive detector consists of sets of plastic scintillator strips and photomultipliers, and they make matrix-like segments so that we can detect where muon passes through. Utilizing the muon characteristic of straight passing through detector, we count as muon when we can connect pass points of each position-sensitive detector by a straight line.

We focus on 'fake track' as a noise source: electromagnetic particles such as gamma rays and electrons generated above the muon detector can simultaneously pass through each position-sensitive detector and make a track as if muon comes from a target. This noise would be reduced with use of more position-sensitive detectors.

We will report simulation result how fake tracks are reduced as number of position-sensitive detector changes by combining cosmic ray simulation and reconstruction of muon detector on computer.